

The Relationship between Vertical, Diapycnal, and Isopycnal Velocity and Mixing in the Ocean General Circulation

S. L. BENNETT

MIT-WHOI Joint Program,* Woods Hole Oceanographic Institution, Woods Hole, MA 02543

(Manuscript received 15 March 1985, in final form 29 July 1985)

ABSTRACT

On ocean general circulation scales, vertical velocity w is extremely small, $O(10^{-5})$ smaller than the horizontal velocity in scale. Nevertheless, it is of great importance to advective-diffusive and vorticity balances. In order to better understand the relationship between the cross-isopycnal (diapycnal) velocity, the mixing, and w , in a nonideal ocean in which some mixing and density sources are present, the velocity vector is decomposed into isopycnal and diapycnal components. Applying this decomposition to the exact continuity (mass conservation) equation, it is shown that while the diapycnal divergence is in principle the first correction to the isopycnal divergence for general circulation scales, the observational uncertainties in the isopycnal velocity are large enough that the diapycnal divergence cannot in practice be determined. Using these results, the horizontally averaged near-vertical (diapycnal) velocity computed by Wunsch et al. in a model of the South Pacific (28–43°S) is reconsidered. It is shown that the calculation of diapycnal velocity from isopycnal mass convergence is not consistent with uncertainties in the isopycnal velocity and that the implied mixing cannot be accounted for with simple diffusion models and salt-fingering alone.

1. Introduction

What is the precise relationship between the vertical velocity (normal to geopotentials) and the cross-isopycnal (diapycnal) velocity in the large-scale time-mean ocean general circulation?

One extreme possibility is that they are completely unrelated. For example, in the β -spiral method of Stommel and Schott (1977) in its simplest form, diapycnal flow is assumed to be identically zero. Then, if the relative vorticity is small compared to the planetary vorticity, a small, nonzero vertical velocity divergence must be present to provide vortex stretching wherever the fluid moves across planetary vorticity contours, in order to conserve absolute vorticity.

The other extreme possibility is that the vertical and diapycnal velocities are nearly equal. This was assumed by Wunsch et al. (1983; hereafter referred to as WHG), in their application of inverse methods to the Scorpio trans-Pacific sections at 28 and 43°S. Having made this assumption, they compute a horizontally averaged near-vertical velocity \bar{w} that is downward throughout the water column.

How are the isopycnal velocity and mass flux divergences related to the diapycnal velocity and mass flux divergences and to the potential density sources, e.g., mixing? The answer to this question bears upon the computation of the diapycnal velocity from the isopycnal mass flux divergence, as was done in WHG.

The decomposition of the velocity \mathbf{u} into an isopycnal component \mathbf{u}_a and a diapycnal component \mathbf{u}_c (a for “along,” c for “cross”) is a natural one in the ocean since the physics (scales and momentum balances) and magnitude of \mathbf{u}_a and \mathbf{u}_c are quite different. Typically \mathbf{u}_a is associated with potential density-conserving large-scale dynamical balances, e.g., the wind-driven circulation, while \mathbf{u}_c is associated with small-scale mixing processes such as internal wave breaking, salt-fingering, lateral (isopycnal) mixing and the resulting cabbelling, and convection. These mixing processes vary in intensity from place to place in the ocean; isopycnals are thought to leak most in such special subregions of the ocean as surface, side, and bottom boundary layers, density fronts, mode and deep water formation sites, outflows from marginal seas, and near strong currents (e.g., the Pacific Equatorial Undercurrent).

Away from such special regions (and sometimes within them), in the ocean interior, \mathbf{u}_c is indeed much smaller than \mathbf{u}_a . The canonical scale for diapycnal flow is $O(10^{-5} \text{ cm s}^{-1})$ (Munk, 1966; Worthington, 1969; Carmack and Foster, 1975; reviewed by Gargett, 1984), while \mathbf{u}_a even in the deep ocean is $O(1 \text{ cm s}^{-1})$.

An informal decomposition of \mathbf{u} into isopycnal and diapycnal components was first used by Wüst (1935, p. 3), who noted the similarity of the temperature-salinity (T - S) relationship across the horizontal free surface to the T - S relationship across the vertical span of the thermocline and deep water. He took this as evidence for advection predominantly along density surfaces and attributed variations in density along presumed flow paths to mixing.

* WHOI Contribution 5901.

Analysis of hydrographic data on the basis of flow along isentropic (constant potential density, isopycnal) surfaces was subsequently introduced by Montgomery (1938), in an extension of Shaw's (1930, pp. 259-264) introduction of isentropic weather maps as a meteorological tool.

The idea of strong isopycnal flow, accompanied by weak diapycnal flow (which can therefore be neglected in some contexts), is by now a common one in general circulation oceanography. The recent thermocline theories of Luyten et al. (1983) and Rhines and Young (1982), for example, are founded on this premise.

Recently, investigators interested in the effects of mixing on seawater have made use of a local isopycnal coordinate system. Redi (1982) used a local coordinate rotation to relate an isopycnal diffusivity tensor \mathbf{K}^I with only diagonal terms to a geopotential $[x, y, z(p)]$ tensor \mathbf{K}^g with nonzero off-diagonal terms. McDougall (1984) derived an equation for the rate of change of potential temperature on a potential density surface from the potential density equation in isopycnal coordinates; this equation may be rewritten in terms of a relationship between the diapycnal velocity and the mixing.¹

A local isopycnal coordinate system based on a rotation of coordinate axes does not, however, lead to expressions for the gradient, divergence, and curl operators. These operators have terms proportional to the variation in length (h_x, h_y, h_r) of the local isopycnal orthogonal basis vectors ($\mathbf{x}', \mathbf{y}', \mathbf{r}'$). The length variation arises from the global (meso- or general-circulation scale) properties of the coordinate system such as the variation of isopycnal tilt and static stability from place to place.

To illustrate the effect of variations of h , consider the variation of h_ϕ for cylindrical (r, ϕ, z) coordinates. The azimuthal basis vector ϕ has length $h_\phi = r$, where r is the distance from the origin, and the gradient operator in cylindrical coordinates reflects this:

$$\text{grad} = \mathbf{r}1/rd/dr + \phi1/rd/d\phi + \mathbf{k}d/dz \quad (1)$$

where carets indicate unit vector. An accurate expression for the divergence operator is necessary if the net flux into a volume is to be related to the net flux out of it.

2. Isopycnal and diapycnal components of velocity

The velocity \mathbf{u} may be formally decomposed into isopycnal and diapycnal components.

First define the following density parameters:

$\rho(p, \theta, s)$	in situ density
ρ_0	in situ density, mean value (const, $\approx 1000 \text{ kg m}^{-3}$)
$\rho'(p, \theta, s) = \rho - \rho_0$	in situ density, departure from mean value
$\rho_s(p(z))$	in situ density, mean vertical profile, (used for expanding in mean isobaric coordinates plus departures)
$\sigma_{pr}(\theta, s) = \rho(p_r, \theta, s)$	potential density referenced to p_r
$\Delta\rho(p, \theta, s) = \rho - \sigma_{pr}$	adiabatic density correction.

The notation () for total, (subscript s) for mean vertical, (') for anomalies and (prefix Δ) for adiabatic correction effects, will be used in some subsequent thermodynamic definitions; θ is potential temperature and s is salinity. Symbols in capital letters or square brackets represent the scale of the same symbol in small letters, e.g., U or $[u]$ represents the scale of u . Here σ_{pr} always refers to the total potential density (e.g., 1027.2 kg m^{-3}) even though numerical values for σ_{pr} are given in sigma units (e.g., 27.2), following common practice.

Now decompose the velocity vector as follows:

$$\mathbf{u} = \mathbf{u}_a + \mathbf{u}_c \quad (2)$$

$$\mathbf{u}_c \times \text{grad}\sigma_{pr} = 0 \quad (3)$$

$$\mathbf{u}_a \cdot \text{grad}\sigma_{pr} = 0 \quad (4)$$

$$\mathbf{u}_c \cdot \text{grad}\sigma_{pr} = J \quad (5a)$$

$$J = D\sigma_{pr}/Dt - \partial\sigma_{pr}/\partial t. \quad (5b)$$

Equations (2)–(4) simply say that \mathbf{u}_a is perpendicular to the density gradient everywhere, \mathbf{u}_c is parallel to it, and that their sum is \mathbf{u} . The \mathbf{u}_c and \mathbf{u}_a are identical to the velocity components obtained from a local coordinate rotation which aligns \mathbf{k} with $\text{grad}\sigma_{pr}$.

Equations (5a, b) define J as the advective part of any potential density sources. For steady flow, J is zero when the salt and heat fluxes into a water parcel are individually zero; or, when the salt and heat buoyancy fluxes computed at p_r are equal and opposite.

These equations are just enough to define \mathbf{u}_a and \mathbf{u}_c uniquely in terms of \mathbf{u} and J . Define the isopycnal slopes h_x, h_y

$$h_x = -(\sigma_{pr})_x/(\sigma_{pr})_z, \quad h_y = -(\sigma_{pr})_y/(\sigma_{pr})_z \quad (6a,b)$$

$$\text{grad}(\sigma_{pr}) = -\hat{i}h_x(\sigma_{pr})_z - \hat{j}h_y(\sigma_{pr})_z + \hat{k}(\sigma_{pr})_z. \quad (7)$$

Then, (3) and (4) give

$$v_c = -h_y w_c, \quad u_c = -h_x w_c \quad (8a,b)$$

$$-(h_x u_a + h_y v_a) + w_a = 0 \quad (9)$$

so that (5) becomes

$$(h_x^2 + h_y^2 + 1)w_c = J/(\sigma_{pr})_z. \quad (10)$$

¹ The diapycnal velocity used by McDougall is defined locally at each point $[x, y, p(z)]$ as the velocity normal to surfaces of constant σ_{pr} , potential density referenced to a pressure p_r , with $p_r = p$. Diapycnal velocity as defined below in this paper, is normal to surfaces of constant σ_{pr} , $p_r = \text{const}$.

Solving for \mathbf{u}_a in terms of J , $\text{grad}\sigma_{pr}$, and \mathbf{u} ,

$$u_a = u + h_x J / [(\sigma_{pr})_z (h_x^2 + h_y^2 + 1)] \quad (11a)$$

$$v_a = v + h_y J / [(\sigma_{pr})_z (h_x^2 + h_y^2 + 1)] \quad (11b)$$

$$w_a = w - J / [(\sigma_{pr})_z (h_x^2 + h_y^2 + 1)]. \quad (11c)$$

These expressions are exact.

3. Discussion: Oceanic vertical velocity

In the ocean, isopycnals slope gently ($h_x, h_y \ll 1$). When h_x and h_y are small, Eqs. (11) are anisotropic, in the following sense. From (10), $w_c \sim J / (\sigma_{pr})_z$. Since $W \ll (U, V)$ (the flow has a horizontal component to lowest order), the approximations $u \sim u_a$ and $v \sim v_a$ from (11a, b) are correct for the horizontal component of velocity. The approximation for the vertical component of velocity presents several choices. Taking $w \sim w_a$ (as in the β -spiral method) is correct only if $W_a \gg W_c$. Otherwise, either $w \sim w_c$ (as in WHG) for $W_a \ll W_c$; or $w = w_c + w_a$ for $W_c \sim W_a$ (neither term can be neglected in favor of the other).

Although the vertical velocity components w_a and w_c and their sum w are difficult if not impossible to measure in the ocean, together or separately, they are indeed physically distinct entities. For example, at the (horizontal) free surface of a flow being heated from above ($w_c > 0$), fluid must cross sloping isopycnal surfaces ($w_a < 0$) flowing horizontally ($w = 0$).

Similar (partial?) cancellation may occur near the bottom boundary of the ocean in tongues of dense water. The Antarctic Bottom Water tongue in the North

Atlantic, discussed by Whitehead and Worthington (1982), is defined by isopycnals sloping into the ocean floor ($w_a < 0$), from which water might exit nearly horizontally as it entrains (mixes turbulently with, $w_c > 0$) lighter water from above.

Where w_c and w_a have the same sign, they complement each other. The equatorial undercurrent structure proposed by Bryden and Brady (1985) has isopycnal zonal flow along shoaling isopycnals ($w_a > 0$), augmented by upward diapycnal flow ($w_c > 0$). Another example is Worthington's (1972) theory of anticyclonogenesis as a result of winter outbreaks of polar air over subtropical gyres. Here, surface cooling ($w_c < 0$) may complement Ekman convergence ($w_a < 0$), thus enhancing the anticyclonic wind-driven circulation.

4. Discussion: Mixing and the direction of flow relative to isopycnals

It is instructive to relate J and \mathbf{u} by a slightly different (and more usual) method (Fig. 1). Between \mathbf{u} and $\text{grad}\sigma_{pr}$ an angle ϕ is formed such that

$$\mathbf{u} \cdot \text{grad}\sigma_{pr} = |\mathbf{u}| |\text{grad}\sigma_{pr}| \cos\phi = J \quad (12)$$

(with $0 \leq \phi < \pi$). Equation (12) is a restatement of (5). Let $\gamma = \phi - \pi/2$; γ is the angle made by \mathbf{u} and the local isopycnal tangent plane. Then $\cos\phi = -\sin\gamma$. For purely isopycnal flow, $\gamma = 0$.

For flow crossing isopycnals very obliquely so that $\gamma \ll 1$, $-\sin\gamma \sim -\gamma$. For gently sloping isopycnals, $|\text{grad}\sigma_{pr}| \sim -(\sigma_{pr})_z$. In the presence of both of these conditions, $|\mathbf{u}| \sim |\mathbf{u}_H|$, where \mathbf{u}_H is the horizontal velocity. Thus

$$J \sim |\mathbf{u}_H| (\sigma_{pr})_z \gamma. \quad (13)$$

The isopycnal tangent plane and the horizontal plane make an angle ω such that $w_a = |\mathbf{u}_a| \sin\omega$, and $w_c = |\mathbf{u}_c| \cos\omega$. Between \mathbf{u} and the horizontal plane an angle ν is formed, such that $w = |\mathbf{u}| \sin\nu$.

Now $\gamma = \nu - \omega$, which may be substituted directly into (13); $w_c = w - w_a$ and $\gamma = \nu - \omega$ are equivalent statements.

From measurements of the density field J , γ , and \mathbf{u} can be determined if simplifying assertions are first made about the dynamics and the functional form of J . Schott and Zantopp (1980) and Olbers et al. (1982) restricted the form of J to depend on n parameters and the density field, and assumed thermal wind and linearized vorticity dynamics; this made it possible to solve for the n parameters, \mathbf{u} , and (implicitly) γ by simultaneous linear regression using scalar, e.g., density, gradient data at $N \geq (n + 3)$ depths.

5. Mass conservation and the divergence of \mathbf{u}_a and \mathbf{u}_c

No matter how different the physics and magnitude of \mathbf{u}_a and \mathbf{u}_c are, the two components are always linked by the continuity (mass conservation) equation

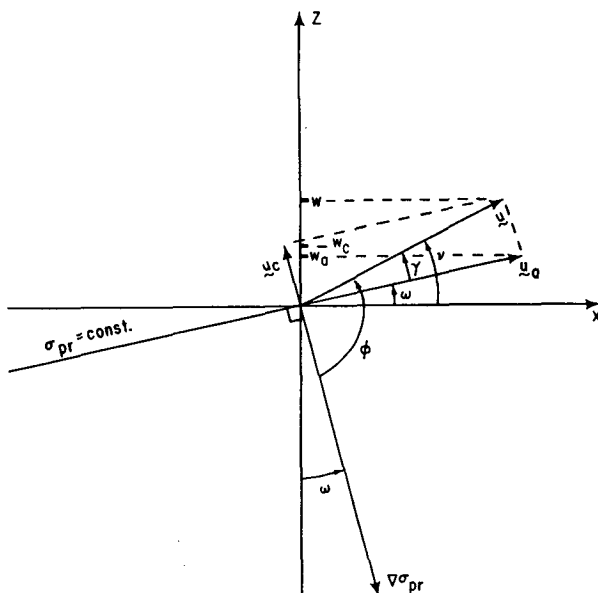


FIG. 1. Sketch of \mathbf{u} , \mathbf{u}_a , \mathbf{u}_c , $\text{grad}\sigma_{pr}$, and angles.

$$\partial\rho/\partial t + \text{div} \cdot \rho \mathbf{u} = 0 \quad (14)$$

which is exact. The continuity equation is quite different from the in situ density equation

$$D\rho/Dt = S_R \quad (15)$$

in which S_R represents sources of ρ . In fact, (14) may be rewritten

$$\text{div} \cdot \mathbf{u} = \rho^{-1} S_R. \quad (16)$$

When two or more of (U/X , V/Y , W/Z) are much greater than $\rho^{-1} S_R$, the continuity equation yields the approximate and powerful simplification

$$\text{div} \cdot \mathbf{u} = 0 \quad (17)$$

known as incompressibility. In incompressible flow, the in situ density equation (15) may or may not retain S_R as a lowest-order term, depending on the relative size of S_R compared to ($[\rho']/[t]$, $U[\rho']/X$, $V[\rho']/Y$, $W[\rho']/Z$).

Precisely because of the opportunity for confusion presented by these scaling arguments, it is desirable to return to the exact continuity equation (14) and rewrite it using (5),

$$\begin{aligned} \text{div} \cdot \mathbf{u}_a &= -[\text{div} \cdot \mathbf{u}_c + \rho^{-1}(D\sigma_{pr}/Dt + D\Delta\rho/Dt)] \\ &= -[\text{div} \cdot \mathbf{u}_c + \rho^{-1}(J + \partial\sigma_{pr}/\partial t + D\Delta\rho/Dt)] \end{aligned} \quad (18)$$

anticipating an approximation of the form $\text{div} \cdot \mathbf{u}_a = O(\epsilon)$, for flows in which the mixing and pressure effects are $O(\epsilon)$, $\epsilon \ll 1$.

Let the potential temperature and salt equations define S_Q and S_S :

$$D\theta/Dt = S_Q \quad (19)$$

$$Ds/Dt = S_S. \quad (20)$$

The coefficients of thermal expansion $\alpha(p, T, s)$ and $\alpha''(p, \theta, s)$, coefficients of saline contraction $\beta(p, T, s)$ and $\beta''(p, \theta, s)$, and the inverse square sound speed λ are defined by

$$\alpha = -\rho^{-1}(\partial\rho/\partial T)_{p,s} \quad (21a)$$

$$\alpha'' = -\rho^{-1}(\partial\rho/\partial\theta)_{p,s} = \alpha(\partial T/\partial\theta)_{p,s} \quad (21b)$$

$$\beta = \rho^{-1}(\partial\rho/\partial s)_{p,T} \quad (22a)$$

$$\beta'' = \rho^{-1}(\partial\rho/\partial s)_{p,\theta} = \beta + \alpha''(\partial\theta/\partial s)_{p,\theta} \quad (22b)$$

$$\lambda = (\partial\rho/\partial p)_{s,\theta} \quad (23)$$

noting that $(\partial T/\partial\theta)_{p,s} \sim 1$ and $(\beta - \beta'')\beta^{-1} \sim 3 \times 10^{-3}$ (Gill, 1982, p. 54).

For $\rho = \rho(p, \theta, s)$, recalling that $\rho(p_r, \theta, s) = \sigma_{pr}(\theta, s)$, J is

$$\begin{aligned} J &= D\sigma_{pr}/Dt - \partial\sigma_{pr}/\partial t \\ &= \sigma_{pr}(-\alpha''_{pr}S_Q + \beta''_{pr}S_S) - \partial\sigma_{pr}/\partial t \end{aligned} \quad (24)$$

where $\alpha''_{pr} = \alpha''(p_r, \theta, s)$ and $\beta''_{pr} = \beta''(p_r, \theta, s)$. Cabbeling (computed at p_r) is included in J , i.e., contributions from the derivatives $\partial^{(m+n)}f_{pr}/\partial t^m \partial s^n \partial \theta^q$, where $f_{pr} = (\alpha''_{pr}, \beta''_{pr})$, $(m, n) \geq 0$, and $(m+n) \geq 1$. The pressure correction (not necessarily small) to this reference pressure cabbeling comes in below. The time-dependent term is retained for completeness despite the immediate interest in a time-mean flow.

First consider the continuity equation (18) for a fluid in which $\Delta\rho$, the difference between in situ density ρ and potential density σ_{pr} , varies only with p :

$$\text{div} \cdot \mathbf{u}_a = -[\text{div} \cdot \mathbf{u}_c + \rho^{-1}(J + \partial\sigma_{pr}/\partial t) - wg\lambda]. \quad (25)$$

If the hydrostatic approximation ($dp \sim -\rho g dz$) may be used, the $-wg\lambda$ term may be incorporated into the divergence operator by the use of isobaric coordinates, (e.g., see Holton, 1979, pp. 54–56), giving without further approximation

$$\text{div}_p \cdot \mathbf{u}_a = -[\text{div}_p \mathbf{u}_c + \rho^{-1}(J + \partial\sigma_{pr}/\partial t)] \quad (26)$$

$$\text{div}_p = (\partial/\partial x)_{y,p} + (\partial/\partial y)_{x,p} + (g\rho)^{-1} \partial/\partial z(\rho g). \quad (27)$$

For seawater, in which $\Delta\rho$ varies with (p, θ, s) , the continuity equation can be written using the terms of (26), plus new terms. First write

$$\begin{aligned} D\Delta\rho/Dt &= (D\rho/Dt - D\sigma_{pr}/Dt) \\ &= \rho(-\alpha''S_Q + \beta''S_S - wg\lambda) \\ &\quad - \sigma_{pr}(-\alpha''_{pr}S_Q + \beta''_{pr}S_S). \end{aligned} \quad (28)$$

Define $\Delta_{pr}\alpha'' = \alpha'' - (\rho^{-1}\sigma_{pr})\alpha''_{pr}$ and $\Delta_{pr}\beta'' = \beta'' - (\rho^{-1}\sigma_{pr})\beta''_{pr}$. Then the continuity equation can be written

$$\begin{aligned} \text{div} \cdot \mathbf{u}_a &= -[\text{div} \cdot \mathbf{u}_c + \rho^{-1}(J - \partial\sigma_{pr}/\partial t) \\ &\quad - S_Q\Delta_{pr}\alpha'' + S_S\Delta_{pr}\beta'' - wg\lambda] \end{aligned} \quad (29)$$

which in isobaric coordinates is

$$\begin{aligned} \text{div}_{ps} \cdot \mathbf{u}_a &= -[\text{div}_{ps} \cdot \mathbf{u}_c + \rho^{-1}(J + \partial\sigma_{pr}/\partial t) \\ &\quad - S_Q\Delta_{pr}\alpha'' + S_S\Delta_{pr}\beta'' - wg\lambda'] \end{aligned} \quad (30)$$

where $\lambda = \lambda_s(p(z)) + \lambda'$ and $dp_s = -\rho_s g dz$.

The first three terms on the rhs of (30) and the p_s coordinates are analogous to the terms in (26). The remaining three new terms, which are not necessarily small, all come from the cross-derivatives $\partial^{(m+n+q)}f/\partial p^m \partial s^n \partial \theta^q$, $f = (\alpha'', \beta'')$, $m \geq 1$, $(n, q) \geq 0$. The $\Delta_{pr}\alpha''$ and $\Delta_{pr}\beta''$ terms include the pressure corrections to the reference-pressure thermal expansion ($f = \alpha''$, $m \geq 1$, $n = 0$, $q = 0$), saline contraction ($f = \beta''$, $m \geq 1$, $n = 0$, $q = 0$), and cabbeling [$f = (\alpha'', \beta'')$, $m \geq 1$, $n > 0$ and/or $q > 0$]. The λ' term accounts for any sound-speed anomalies remaining after the mean $\lambda_s(z)$ profile has been incorporated into div_{ps} .

a. Special cases

For steady flow in which S_Q and S_S are both zero, the isopycnal divergence is balanced by $D\Delta\rho/Dt$, which is $-wg\lambda$ for hydrostatic flow. The diapycnal velocity and thus the diapycnal divergence are identically zero. Flow is confined to isopycnal sheets $d\sigma_{pr} = \text{const}$, of variable thickness $d\sigma_{pr}/|\text{grad}\sigma_{pr}|$.

If $D\Delta\rho/Dt$ is also zero, then ρ is constant and consequently the isopycnal divergence is zero. In this trivial case and this case alone the diapycnal and isopycnal divergences are exactly equal.

b. Scaling considerations

Is there a consistent scaling for which the diapycnal divergence is the largest of the $O(\epsilon)$ terms? In particular, is the diapycnal divergence the first correction to the isopycnal divergence for oceanic scales?

Scales which maximize the rhs $O(\epsilon)$ terms of (29), while remaining within plausible ocean general circulation ranges are shown in Table 1, along with the resulting magnitudes of the terms of (29). For the scales shown, the first correction to the isopycnal divergence is, in principle, the diapycnal divergence.

TABLE 1. Oceanic scaling for the continuity equation.

(a) Basic scales

- $U \sim 10 \text{ cm s}^{-1}$
- $\Delta_E U \sim 0.1 \text{ cm s}^{-1}$
- $L \sim 10^8 \text{ cm}$
- $W_c \leq W$
- $W \sim 10^{-5} \text{ cm s}^{-1}$
- $H \leq 5 \times 10^3 \text{ cm}$
- $N^2 \leq 10^{-5} \text{ s}^{-2}$
- $g = 10^3 \text{ cm s}^{-2}$
- $\lambda_s = 2 \times 10^{10} \text{ cm}^2 \text{ s}^{-2}$
- $\lambda = 5 \times 10^{-12} \text{ s}^2 \text{ cm}^{-2}$
- $[\Delta_{pr}\alpha''] \sim 10^{-4} \text{ }^\circ\text{C}^{-1}$
- $[\Delta_{pr}\beta''] \sim 10^{-5}$
- $[\alpha''_{pr}] \sim (8, 123) \times 10^{-6} \text{ }^\circ\text{C}^{-1} \text{ (min, max)}$
- $[\beta''_{pr}] \sim (7, 8) \times 10^{-4}$

Notes:

- (a) $\Delta_E U$ is an error bar on U
- (b) $N^2(p \sim p_c) = -g\rho^{-1}(\sigma_{pr})_z$
- (c) $[\alpha''_{pr}, \beta''_{pr}, \Delta_{pr}\alpha'', \Delta_{pr}\beta'']$, chosen from Millard (1984) to maximize terms in Eq. (29), for $0 \leq p \leq 4000 \text{ dbars}$, $-2 \leq \theta \leq 20 \text{ }^\circ\text{C}$, and $0.030 \leq s \leq 0.040$.

(b) Derived scales for terms in Eq. (29)

- $\text{div} \cdot \mathbf{u}_a \sim U/L \pm \Delta_E U/L \sim 10^{-7} \pm 10^{-9} \text{ s}^{-1}$
- $\text{div} \cdot \mathbf{u}_c \sim W_c/H \sim 2 \times 10^{-11} \text{ s}^{-1}$
- $J/\rho \sim (\sigma_{pr})_z W_c/\rho \sim W_c N^2/g \sim 10^{-13} \text{ s}^{-1}$
- $wg\lambda_s \sim 5 \times 10^{-13} \text{ s}^{-1}$
- $wg\lambda \sim 5 \times 10^{-14} \text{ s}^{-1}$
- $\Delta_{pr}\alpha'' S_Q/\rho \sim \leq 10^{-12} \text{ s}^{-1}$
- $\Delta_{pr}\beta'' S_s/\rho \sim \leq 10^{-15} \text{ s}^{-1}$

c. Effect of errors in \mathbf{u}_a

In practice, any computation of the isopycnal divergence from observational data will produce a residual E , where $E \leq O(\epsilon, \Delta_E U/L)_{\text{max}}$, where $\Delta_E U$ is an error bar on U . Since $U/L \gg E$, E can be chosen to be arbitrarily small (including $E = 0$) without affecting the $O(U/L)$ terms. If E is formally computed to arbitrary order, it will be dominated by the largest of the $O(\epsilon, \Delta U_E/L)$ terms.

This is analogous to determining w_z from $-(u_x + v_y)$ in quasi-horizontal flow when there are observational errors associated with (u, v) . [(u, v, w) are the usual Cartesian velocity components.]

Referring to the Table 1 scales, the diapycnal divergence is $O(10^{-2})$ smaller than the residual isopycnal divergence due to errors in the isopycnal velocity. Similarly, using these same scales the vertical velocity divergence is $O(10^{-2})$ smaller than the residual horizontal divergence.

Are there scales different from those given in Table 1 but within the ranges appropriate for the WHG model results such that the diapycnal divergence W_c/H is as large as the error term $\Delta_E U/L$? Using the Table 1 scales as a starting point, either W_c or L must increase, or $\Delta_E U$ or H must decrease. At 1000 km L is already at least an order of magnitude greater than the Rossby radius and equal to the meridional scale of the South Pacific gyre. The zonal extent of the South Pacific is an order of magnitude larger than this, though property (heat, salt, silicate) convergences are most likely meridional, not zonal.

The $\Delta_E U$ is 0.1 cm s^{-1} , an optimistic error estimate for any point measurement of oceanic velocity. In a box model, where smooth fields of isopycnal velocity and velocity divergence are estimated from a set of point measurements, the total error scale $\Delta_E U$ is the sum of the point measurement error and the estimated error in the field-generating procedure. Thus the point measurement error can be regarded as a lower bound on the total error.

Here, H is 5 km, the full water depth. Since WHG's \bar{w} is $O(W_c)$ and nearly constant throughout the water column, with no evidence of boundary layers or internal variation in \bar{w} on scales much less than this, e.g. 500 m or less, this is an appropriate choice. The W_c has the maximum value reported in WHG.

What about much smaller values of H or much larger values of W_c in the real ocean? From an observational point of view, there is a nearly total absence of direct evidence concerning both the vertical scale of time-averaged diapycnal velocities of gyre-wide horizontal scale, and the maximum scale for these velocities. However, it is usual in scale analysis to produce a simplified set of equations using all known scales plus estimates of any unknown scales, then to require for

consistency that any solution produced from the simplified set of equations not contradict the original scaling. In order to examine the WHG model for such consistency, it is appropriate to choose values for H and W_c that characterize the solution produced by the model.

Using the most promising values ($\Delta_E U \sim 0.1 \text{ cm s}^{-1}$, $L \sim 10^4 \text{ km}$, $W_c \sim 10^{-5} \text{ cm s}^{-1}$, $H \sim 5 \text{ km}$), the diapycnal divergence is still $O(10^{-1})$ smaller than the residual isopycnal divergence due to errors.

Thus, the scales of the WHG results are not consistent with those leading to the isopycnal/diapycnal divergence approximation to the mass conservation equation.

d. Mass flux divergence

Leaving aside the question of errors, consider flows where the second through sixth terms on the rhs of the continuity equation (29) are as large or larger than the diapycnal velocity divergence. For such flows, the continuity equation in mass flux divergence form incorporates these terms directly

$$\partial \rho / \partial t + \text{div} \cdot \rho \mathbf{u}_a = -\text{div} \cdot \rho \mathbf{u}_c. \quad (31)$$

This form of the equation has terms which are more conveniently computed than those of the expanded form (29). However, for flows where the second through sixth terms of (29) are negligible, the mass flux divergence is only negligibly more accurate than the velocity divergence, since the contribution to the mass flux divergence due to in situ density variation is smaller than that from the velocity divergence.

e. Green's theorem and scaling considerations

The relative scales of terms in an equation such as (29) may be altered by application of Green's theorem (Hildebrand, 1976, p. 301), depending on the integral volume used. The WHG model layers and boxes do not appear to have this property; the scales chosen to characterize the relative magnitudes of fluxes for an arbitrary volume seem equally well-suited to characterize the relative magnitudes of fluxes through the surfaces of the WHG boxes and layers.

Examples in the literature where this property of scale alteration does occur include Hall and Bryden's (1982) computation of heat flux across 24°N in the Atlantic, and Toole and Raymer's (1984) similar computation at 32°S in the South Indian Ocean. By choosing basins which are nearly-closed to one side of a hydrographic section (except for small Bering, Banda Strait transport), fluxes and the associated errors are very small on all surfaces except for the hydrographic section. A similar but more sophisticated example from these same studies is the near-elimination of the heat flux due to unknown interior barotropic velocities after

integration over the interior hydrographic stations (see Hall and Bryden, 1982, for a full explanation), not because such a flux is relatively small locally anywhere in the flow, but because of integral constraints specific to this particular type of volume.

6. Ekman pumping

The imposition of a vertical velocity w_e at the surface, or at the base of a surface boundary layer, of a stratified fluid with sloping isopycnals implies a mass flux in or out of those isopycnal sheets which intersect the surface. In an ocean box model, w_e , or equivalently, the convergence in the surface boundary (Ekman) layer, may be prescribed by the modeler based on wind stress observations. If there is no mixing or other sources of θ or s in the model, then w_e is zero everywhere by (5): w_e in the modeled region can feed mass only into those isopycnals which intersect the surface in that same region. Denser layers may of course exchange mass with the surface boundary layer where these layers *do* outcrop, away from the modeled region.

In WHG models S-2, 3, 4, Ekman fluxes across 28 and 43°S are prescribed in Layer 1, the only layer which intersects the ocean surface in the modeled region. These Ekman fluxes are not balanced, so a net convergence in this layer results. This convergence is not required to be balanced exactly by geostrophic flux divergence; it is allowed to be partially balanced by an accumulation of mass in the layer that is then assigned to the diapycnal flow \bar{w} , which flows into layer 2 below. The \bar{w} is w_e averaged over an isopycnal surface of a box. Slight mass residuals are allowed in each successive layer, to be assigned to diapycnal flow into the layer below. The maximum amount of mass residual the model is allowed to produce in each layer is specified a priori. The entire box does conserve mass precisely.

This procedure has two distinct implications. First, as was shown in Section 5, any residual isopycnal convergence should be regarded as due to uncertainties in \mathbf{u} ; it need not be balanced by diapycnal divergence.

Second, diapycnal velocity is accompanied by potential density sources, from (5). Thus the apparent penetration of the Ekman pumping beyond the base of Layer 1 in the WHG model is accompanied by mixing (since external potential density sources, e.g. sunlight, do not penetrate this deeply).

7. Simple diffusion models, salt-fingering, and mixing in the WHG model

Do the values computed by WHG for \bar{w} correspond to diapycnal velocities expected from simple diffusion models or salt-fingering? The purpose of this calculation is only to compare the results of the models; the question of their applicability to the real ocean is not addressed here.

If the buoyancy term J arises from internal wave breaking, then it is customary to define a vertical diffusivity K_v in terms of a Reynolds transport term $-\overline{w'\sigma'_z}$ and the time-mean density field σ_z

$$-\overline{w'\sigma'_z} = (K_v\sigma_z)_z. \tag{32}$$

If there are no other contributions to J , then from (10), assuming $(h_x, h_y) \ll 1$,

$$\overline{w\sigma_z} = (K_v\sigma_z)_z. \tag{33}$$

If K_v is relatively constant with depth,

$$K_v \sim \overline{w\sigma_z}/\sigma_{zz} = \overline{w}N^2/(N^2)_z = -2\overline{w}B/B_z \tag{34}$$

where N ($p = p_r$) is the buoyancy frequency $[-g\rho^{-1}(\sigma_{pr})_z]^{1/2}$, and B is the buoyancy period $2\pi/N$.

Estimates for K_v calculated for some of the WHG layer boundaries using (34), WHG values for \overline{w} , and the Scorpio data (Stommel et al., 1973) are given in Table 2. Throughout the water column \overline{w} is negative. Except for the base of layer 3, B_z and thus K_v are negative. The base of layer 3, $\sigma_0 = 27.20$, is just below the core of the South Pacific Mode Water at $\sigma_0 = 27.00$ – 27.10 (McCartney, 1982). Mode Waters by definition represent maxima in B and, in consequence, overlay isopycnals with positive B_z . Only below the Mode Water, then, are the results of the WHG model consistent with constant K_v , downgradient diffusion acting alone.

Gargett (1984) argues that internal wave breaking may be more accurately modeled by $K_v \sim aN^{-1} = bB$, with $(a, b) = \text{const} > 0$, than by $K_v \sim \text{const}$. Substituting this form for K_v into (33) gives

$$\overline{w} = -bB_z; \tag{35}$$

\overline{w} negative when B_z is negative corresponds to up-gradient diffusion in this model also (but the sign of w_z , of central importance to linear vorticity dynamics, may be altered).

Can salt-fingering produce negative \overline{w} anywhere in the water column? Salt fingering can occur where cold, fresh water underlies warm, salty water. Such conditions exist in the northern and western sectors of the WHG model region from the surface down to the Antarctic Intermediate Water (AAIW) salinity minimum at ~ 1000 m, near the level where B_z reaches a maximum. Where fingering occurs, the cold, fresh, underlying water gains salt, causing it to sink across isopycnals (\overline{w} negative); conversely the warm, salty, overlying water rises (\overline{w} positive). Thus, at and above the AAIW, \overline{w} from the WHG model is consistent in sign with buoyancy sources due to salt-fingering.

Negative \overline{w} is consistent with these simple diffusion models and salt-fingering only at the levels noted. Elsewhere, in the deep water in particular, some additional mechanism is required in order to produce a \overline{w} profile similar to that calculated by WHG.

8. Conclusions

The velocity vector may be decomposed, without resort to isopycnal coordinates, into isopycnal and diapycnal components. Expressions for the vertical velocity in terms of isopycnal and diapycnal components, and for the isopycnal divergence follow, without approximation.

TABLE 2. Diapycnal velocity, stratification, and diapycnal diffusivity.

(1) Layer	(2) ~ Depth (m)	(3) σ_{pr} (kg m ⁻³)	(4) \overline{w} (10 ⁻⁵ cm s ⁻¹)	(5) σ_0 (kg m ⁻³)	(6) B (min)	(7) B_z (10 ⁻⁴ min cm ⁻¹)	(8) Neg. sign, B_z (obs < 0/total obs)	(9) K_v , Eq. (34) (10 ⁻¹ cm ² s ⁻¹)
1								
2	200	$\sigma_0 = 26.80$	-0.7	26.81	26 ± 2	-9.3 ± 2.9	12/14	-0.4 ± 0.1
3	500	$\sigma_0 = 27.00$	-0.6	27.01	45 ± 3	-3.3 ± 3.7	9/14	-1.6 ± 1.1
4	900	$\sigma_0 = 27.20$	-0.6	27.21	35 ± 1	0.7 ± 0.7	6/14	6.0 ± 6.2
6	1200	$\sigma_2 = 36.60$	-0.8	27.41	39 ± 1	-3.6 ± 0.6	14/14	-1.7 ± 0.3
	2100	$\sigma_2 = 36.98$	-0.6	27.75	100 ± 6	-5.6 ± 1.9	11/13	-2.1 ± 0.7

Notes:

(1–4) From WHG:

- (1) Layer number, as in WHG Table 1. Layers deeper than 6 omitted since they are not represented at many of the Scorpio stations used;
- (2) approximate depth of layer boundary, from WHG Table 1;
- (3) density of layer boundary; σ_z is potential density referred to 2000 db; and
- (4) \overline{w} , from WHG Fig. 11a.

(5–9) From Scorpio data, Stommel et al., 1973, stations 3, 13, 29, 39, 49, 59, 69 at 43°S; 89, 99, 109, 119, 129, 139, 148 at 28°S;

- (5) σ_0 chosen to estimate (3) above;
- (6) buoyancy period, minutes, mean and standard deviation of mean;
- (7) vertical derivative of buoyancy period, mean and standard deviation of mean computed by nearly-centered first difference, i.e., difference centered on σ_0 as closely as uneven vertical spacing of data allowed;
- (8) number of observations of B_z less than zero/total number of observations used; and
- (9) K_v computed from Eq. (34), mean and standard deviation of mean.

This procedure suggests an alternative interpretation of the WHG model assumptions and results:

- The (horizontally-averaged) diapycnal velocity and the (horizontally-averaged) vertical velocity are not necessarily nearly equal, even when the density gradient is near-vertical.
- Nonzero diapycnal velocities throughout the water column imply mixing throughout the water column (or an unsteady potential density field).
- For the diapycnal velocities computed by the WHG model, the implied mixing is not consistent with simple models of down-gradient diffusion or salt-fingering, except just below the Mode Water at $\sigma_0 = 27.00\text{--}27.10$.
- In practice, diapycnal divergence can be computed from the isopycnal divergence only when the accuracy in the isopycnal velocity is $\ll O(W_c L/H)$ (and other terms in the mass conservation equation due to variations in density are sufficiently small). Otherwise, any residual isopycnal divergence should be ascribed to the uncertainties in the isopycnal velocity. This is analogous to the difficulty encountered in computing vertical velocity divergence from horizontal velocity divergence when the horizontal velocity field is imperfectly known.

These results confirm the importance of direct measurements of mixing in the ocean, since such information leads directly to estimates of diapycnal velocity without reliance on any relation between isopycnal and diapycnal divergence. Further, the inverse method can assimilate this information as constraints, with appropriate weighting. Diapycnal velocities might contribute significantly to vertical velocities in some oceanic regimes.

Acknowledgments. The author wishes to thank M. S. McCartney for helpful discussions and moral support during the gestation of this idea. The expert editorial guidance of J. M. Toole and R. W. Schmitt is sincerely appreciated. Publication of this paper is supported by the Office of Naval Research, Contract N00014-85-C-0001, NR 083-004.

REFERENCES

- Bryden, H. L., and E. C. Brady, 1985: Diagnostic model of circulation in the equatorial Pacific Ocean. *J. Phys. Oceanogr.*, **15**, 1255–1273.
- Carmack, E. C., and T. D. Foster, 1975: On the flow of water out of the Weddell Sea. *Deep-Sea Res.*, **22**, 711–724.
- Gargett, A., 1984: Vertical eddy diffusivity in the ocean interior. *J. Mar. Res.*, **42**, 359–393.
- Gill, A. E., 1982: *Atmosphere-Ocean Dynamics*. Academic Press, 662 pp.
- Hall, M. M., and H. L. Bryden, 1982: Direct estimates and mechanisms of ocean heat transport. *Deep-Sea Res.*, **29**, 339–359.
- Hildebrand, F. B., 1976: *Advanced Calculus for Applications*. Prentice-Hall, 733 pp.
- Holton, J. R., 1979: *An Introduction to Dynamic Meteorology*. Academic Press, 391 pp.
- Luyten, J. R., J. Pedlosky and H. Stommel, 1983: The ventilated thermocline. *J. Phys. Oceanogr.*, **13**, 292–309.
- McCartney, M. S., 1982: Subtropical Mode Water recirculation. *J. Mar. Res.*, **40**(Suppl.), 427–464.
- McDougall, T. J., 1984: The relative roles of diapycnal and isopycnal mixing on subsurface water mass conversion. *J. Phys. Oceanogr.*, **14**, 1577–1589.
- Millard, R. C., Jr., 1984: International oceanographic tables. *UNESCO Tech. Pap. Mar. Sci.*, (in press).
- Montgomery, R. B., 1938: Circulation in upper layers of southern North Atlantic deduced with use of isentropic analysis. *Pap. Phys. Oceanogr. Meteor.*, **6**, Woods Hole Oceanogr. Inst., 55 pp.
- Munk, W., 1966: Abyssal recipes. *Deep-Sea Res.*, **13**, 707–730.
- Olbers, D. J., J. Willebrand and M. Wenzel, 1982: The inference of ocean circulation parameters from climatological hydrographic data. Unpublished manuscript.
- Redi, M. H., 1982: Oceanic isopycnal mixing by coordinate rotation. *J. Phys. Oceanogr.*, **12**, 1154–1158.
- Rhines, P. B., and W. R. Young, 1982: A theory of wind driven circulation. I. Mid-ocean gyres. *J. Mar. Sci.*, **40**(Suppl.), 559–596.
- Schott, F., and R. Zantopp, 1980: On the effect of vertical mixing on the determination of absolute currents by the beta spiral method. *Deep-Sea Res.*, **27A**, 173–180.
- Shaw, N., 1930: The physical processes of weather. *Manual of Meteorology*, Cambridge University Press.
- Stommel, H., and F. Schott, 1977: The beta spiral and the determination of the absolute velocity field from hydrographic station data. *Deep-Sea Res.*, **24**, 325–329.
- , E. D. Stroup, J. L. Reid and B. A. Warren, 1973: Trans-pacific hydrographic section at latitudes 43°S and 28°S: The *Scorpio* expedition—I. Preface. *Deep-Sea Res.*, **20**, 1–7.
- Toole, J., and M. E. Raymer, 1984: Heat and fresh water budgets of the Indian Ocean revisited. *Deep-Sea Res.*, (in press).
- Whitehead, J. A., Jr., and L. V. Worthington, 1982: The flux and mixing rates of Antarctic Bottom Water within the North Atlantic. *J. Geophys. Res.*, **87**, 7903–7924.
- Worthington, L. V., 1969: An attempt to measure the volume transport of Norwegian Sea overflow water through the Denmark Strait. *Deep-Sea Res.*, **16**(Suppl.), 421–432.
- , 1972: Anticyclogenesis in the oceans as a result of outbreaks of continental polar air. *Studies in Physical Oceanography—A Tribute to Georg Wüst on his 80th birthday*, **1**, A. L. Gordon, Ed., Gordon & Breach, 169–178.
- Wunsch, C., D. Hu and B. Grant, 1983: Mass, heat, salt and nutrient fluxes in the South Pacific Ocean. *J. Phys. Oceanogr.*, **13**, 725–753.
- Wüst, G., 1935: Schichtung und Zirkulation des Atlantischen Ozeans. Die Stratosphäre. *Wiss. Ergebn. Dtsch. Atlant. Exped. Meteor.*, **6**, Teil 1, No. 2, 109–288. [English translation, *The Stratosphere of the Atlantic Ocean*, W. J. Emery, Ed., Amerind, New Delhi, 112 pp.]